



Contents lists available at ScienceDirect

Chinese Chemical Letters

journal homepage: [www.elsevier.com/locate/ccllet](http://www.elsevier.com/locate/ccllet)

## Benzothiophene and benzosulfone fused pyrazino[2,3-g]quinoxaline: Synthesis and semiconducting properties



Fangwei Ding<sup>a</sup>, Debin Xia<sup>a,\*</sup>, Xiping Ding<sup>a</sup>, Ruibin Deng<sup>a</sup>, Congwu Ge<sup>b</sup>, Yulin Yang<sup>a</sup>, Ruiqing Fan<sup>a</sup>, Kaifeng Lin<sup>a,\*</sup>, Xike Gao<sup>b,\*</sup>

<sup>a</sup> MIIT Key Laboratory of Critical Materials Technology for New Energy Conversion and Storage, School of Chemistry and Chemical Engineering, Harbin Institute of Technology, Harbin 150001, China

<sup>b</sup> Key Laboratory of Synthetic and Self-Assembly Chemistry for Organic Functional Molecules, Shanghai Institute of Organic Chemistry Chinese Academy of Sciences, Shanghai 200032, China

### ARTICLE INFO

#### Article history:

Received 4 November 2021

Revised 26 November 2021

Accepted 15 February 2022

Available online 19 February 2022

#### Keywords:

Azaarenes

Deep LUMO levels

n-type

Organic semiconductor

Polycyclic aromatic hydrocarbons

### ABSTRACT

A novel air-stable n-type benzothiophene endcapped azaarene (**BTPQ**) and its sulfonated derivative (**BSPQ**) were prepared via two pathways and characterized by NMR, UV-vis, fluorescence and cyclic voltammetry spectroscopy. Symmetrically introducing four nitrogen atoms into acenes, the semiconductor properties could be changed from p-type to n-type detected through the space charge limited current (SCLC) method. After sulfonation of **BTPQ**, **BSPQ** is with deeper frontier orbital energy levels and enhanced the electron mobility.

© 2022 Published by Elsevier B.V. on behalf of Chinese Chemical Society and Institute of Materia Medica, Chinese Academy of Medical Sciences.

Azaarenes (azaacenes) play an important role in organic field-effect transistors (OFETs), organic light-emitting diodes (OLEDs) and organic photovoltaics (OPVs) [1–15], especially those with p-type behaviors have been deeply studied. However, n-type small molecule semiconductors are still developing slowly owing to the lack of effective structural units and the high lowest unoccupied molecular orbital (LUMO) levels hindered the injection of electrons [16,17]. These factors also led to a significant slowdown in n-type semiconductors based on polycyclic aromatic hydrocarbons (PAHs) [18–20]. As far as we know, there are few reports on the synthesis of n-type azaacenes (azaarenes) [21]. In general, the n-type semiconductor needs deep frontier orbital energy levels, so how to effectively reduce frontier orbital energy levels becomes the key to construct n-type materials. The LUMO with  $-4$  eV or lower is commonly required to reduce the electron injection barrier and further profit to match with the metal electrode and stabilize the injected electrons [12–24]. Moreover, the synthesis of n-type semiconductors with high stability is of great significance for the device. Therefore, it is particularly urgent to develop n-type organic semiconductor materials with high stability and deep LUMO levels. Based on our previous work [25,26], herein we present two strate-

gies to build n-type azaarenes by introducing nitrogen atoms and sulfonyl groups (Fig. 1).

As is known to all, the number and position of nitrogen atoms in the molecular skeleton have a significant influence on the semiconductor properties and carriers of the materials [8]. With the increase of the number of nitrogen atoms, the stability of the azaarenes (azaacenes) would also be enhanced. However, bent azaarenes show better stability than linear azaacenes for one more Clar sextet. In addition, it is very important to select the appropriate skeleton to satisfy the delicate balance between solubility and carrier for the purpose of maximum  $\pi$  delocalization [27–29].

Considering the above factors, the anthracene core with good electron delocalization is chosen as the skeleton structure unit, and triisopropylsilyl groups (TIPS) are attached to increase the solubility of the materials. Four nitrogen atoms are subsequently introduced into the target molecule to modulate the molecular energy level and stabilize the molecular structure to meet the energy level requirements of n-type semiconductors. It is worth noting that there are three Clar sextets in the molecular structure, which would also increase molecular stability [30,31]. Besides the sulfonyl group is also brought into the skeleton in this work, so that the lower LUMO levels could be formed and more facilitated to the electron injection.

The synthetic routes are shown in Scheme 1. Target product benzothiophene fused pyrazino[2,3-g]quinoxaline (**BTPQ**) was ob-

\* Corresponding authors.

E-mail addresses: [xia@hit.edu.cn](mailto:xia@hit.edu.cn) (D. Xia), [linkaifeng@hit.edu.cn](mailto:linkaifeng@hit.edu.cn) (K. Lin), [gaoxk@mail.sioc.ac.cn](mailto:gaoxk@mail.sioc.ac.cn) (X. Gao).

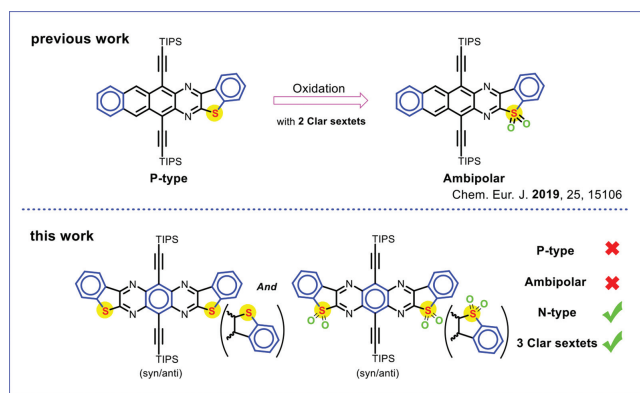
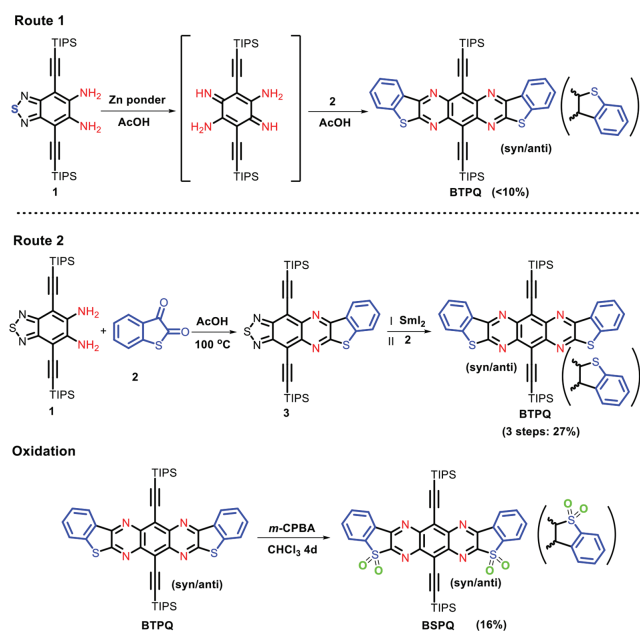


Fig. 1. Molecular structures of bent azaarenes.



Scheme 1. Synthesis of the target products.

tained *via* one step with a low yield (<10%), which could not meet the need of later functionalization and device testing, thus an alternative synthesis route had been developed. Firstly, the intermediate product **3** was synthesized by a condensation reaction [26], subsequently the thiadiazolyl unit was reduced through  $\text{Sml}_2$ . Finally, the product **BTPQ** was obtained once more by a condensation reaction, the total yield of the three steps was increased to 27%. The **BTPQ** is a mixture of isomers and *syn:anti* = 1:1 through the analysis of  $^1\text{H}$  and  $^{13}\text{C}$  NMR (Fig. S2 in Supporting information). The isomers are difficult to separate for their similar physical and chemical properties [32]. Additionally, sulfonated product **BSPQ** was given through oxidation of **BTPQ** with excess *m*-CPBA, since the sulfonyl group can effectively reduce the energy levels.

Product **BTPQ** is orange under sunlight and emits yellow-red fluorescence. **BSPQ** is light red in sunlight, and the color of **BSPQ** is deeper than **BTPQ** under UV (365 nm, Fig. 2). To further study the optical properties of target products, **BTPQ** and **BSPQ** were also investigated in detail by UV-vis absorption and fluorescence spectroscopy. Compared with **ABBT** reported by Anthony's group [33], **BTPQ** imported four nitrogen atoms symmetrically into the skeleton. It could be clearly found that the spectral peaks of **BTPQ** were widened and the peak intensity was redistributed, especially that showed a strong peak at 400–500 nm [34,35]. In addition, it was also found that the  $\lambda_{\text{max}}$  of **BTPQ** had a remarkable red shift of

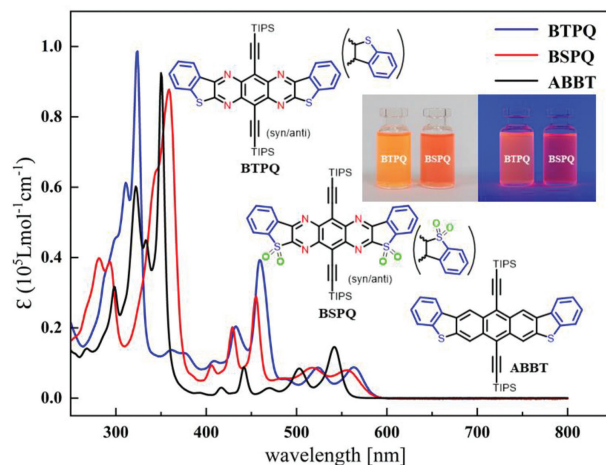


Fig. 2. Absorption spectra of target products in  $\text{CH}_2\text{Cl}_2$ .

21 nm compared with **ABBT**, widening the spectra. Meanwhile, the bandgap value of **BTPQ** decreased from 2.22 eV (**ABBT**) to 2.12 eV, it suggested that doped strategy significantly reduces the optical gap value (Table 1).

As for **BSPQ** with two electron-withdrawing sulfonyl groups, the  $\lambda_{\text{max}}$  showed a slight blue shift compared with **BTPQ**. It may be because that the thiophene ring has relatively better planarity than the sulfonyl ring, which weakened the conjugation degree of **BSPQ**. Furthermore, the electron-deficient sulfonyl group could validly increase the optical gap. The optical gap of molecule **BSPQ** was 2.13 eV (Table 1), and 0.01 eV was more than **BTPQ**, which also revealed that the stability was improved to a certain extent [36]. The fluorescence spectra of target products were showed in Fig. S1 (Supporting information), they both showed two emission peaks, the emission peaks of **BSPQ** were slightly bathochromic than **BTPQ**.

To gain a deep understanding of the electronic behavior of target products, cyclic voltammetry (CV) and differential pulse voltammetry (DPV) experiments were conducted at room temperature. The results were shown in Fig. 3. Within the electrochemical window of  $\text{CH}_2\text{Cl}_2$ , the target products exhibited electron-deficient characteristics. **BTPQ** and **ABBT** both showed multiple reduction peaks [33], the first reduction potentials were  $-1.10\text{V}$  and  $-1.68\text{V}$  (relative to ferrocene), respectively. The corresponding LUMO values were  $-3.70\text{eV}$  and  $-3.12\text{eV}$ . The above results depicted that the introducing nitrogen atom increased the reduction potential and reduced the LUMO energy level, which was more facilitated to electron injection. Moreover, the LUMO level below  $-3.7\text{eV}$  could also avoid the reduction of  $\text{H}_2\text{O}$  [23]. As for their oxidation potentials, the first oxidation potentials of **BTPQ** and **ABBT** were 1.01 V and 0.55 V, respectively, indicating that the **BTPQ** had relatively high antioxidant capacity. Furthermore, the corresponding HOMO values were  $-5.81\text{eV}$  and  $-5.35\text{eV}$ , respectively, the HOMO level

Table 1  
The optical and parameters of the target products.

Product	$\lambda_{\text{max}}$ (nm)	$\lambda_{\text{em}}$ (nm)	$E_{\text{LUMO}}^{\text{a/b}}$ (eV)	$E_{\text{HOMO}}^{\text{a/b}}$ (eV)	$E_{\text{g}}^{\text{c}}$ (eV)	Gap <sup>d</sup> (eV)
<b>BTPQ</b>	563	582	$-3.70/-3.38$	$-5.81/-5.79$	2.11	2.12
<b>BSPQ</b>	556	588	$-4.10/-3.99$	$-6.23/-6.44$	–	2.13
<b>ABBT</b>	542	548	$-3.12/-$	$-5.35/-$	2.23	2.22

<sup>a</sup> Experimental results.

<sup>b</sup> DFT calculated results.

<sup>c</sup> Obtained by CV curves.

<sup>d</sup> Obtained by UV-vis absorption spectra.

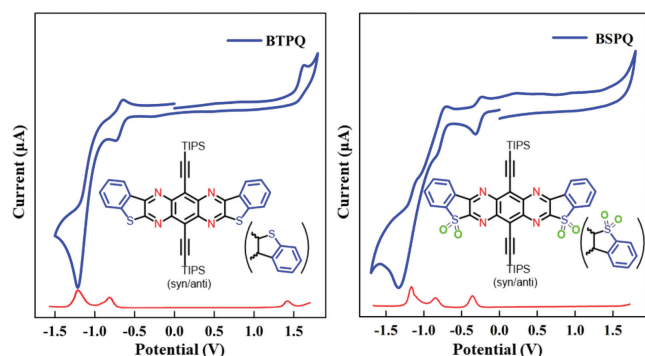


Fig. 3. The CV and DPV curves of target products in  $\text{CH}_2\text{Cl}_2$  and 0.1 mol/L  $\text{Bu}_4\text{NPF}_6$  on a Pt electrode at a scan rate of 50 mV/s vs. Ag/AgCl.

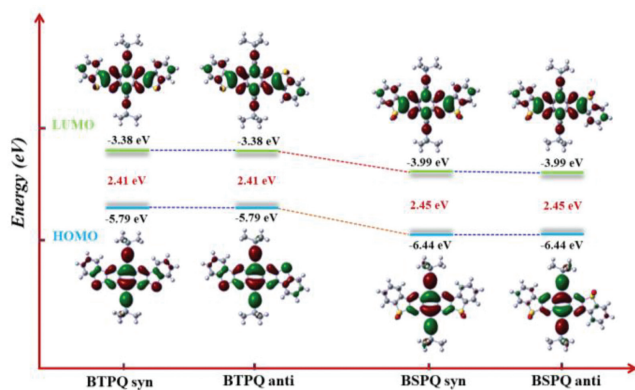


Fig. 4. Frontier molecular orbital diagram of target products.

also shows the same downward trend as the LUMO level. The lower HOMO levels could also enhance oxidation stability and further hinder the hole injection from metal electrode to semiconductor layer, which was very important for photoelectric devices. Compared with **BTPQ**, sulfonated product **BSPQ** had more reduction peaks, showing three reversible reduction peaks. The first reduction potential of compound **BSPQ** was  $-0.70\text{ V}$  (relative to ferrocene), and the corresponding LUMO energy level was  $-4.10\text{ eV}$ , which had already been very low due to the electron-withdrawing sulfonyl group. It also reflected that **BSPQ** could significantly reduce the influence of  $\text{O}_2$ , and elevate the stability of molecules in the air [37]. Besides, from the perspective of frontier orbital energy levels, **BSPQ** might be a potential n-type semiconductor material.

Density functional theory (DFT) calculations were further performed for all target products with Gaussian 09 software and B3LYP 6-311++G\*\* basis set [38,39]. The results were exhibited in Fig. 4. In the process of DFT calculation, isopropyl on silicon was replaced by methyl, and the calculated energy level and geometry of isomer products were similar. The HOMO-LUMO energy level distribution all presented centrosymmetric or axisymmetric arrangement, and the LUMO orbitals possessed highly delocalized electron distribution covered the whole molecular skeleton, and were not limited to the electron-withdrawing part. While the HOMO orbitals mainly located in the tetraazaanthracene part and slightly diffused to the bent phenyl part. The simulation results also revealed that sulfonation had an obvious effect on the frontier orbital energy level, the HOMO/LUMO energy levels decreased evidently with bandgap increasing, which were consistent well with the absorption spectral data. In addition, the thermal behavior was conducted with thermogravimetric analysis (TGA). As depicted in Fig. S6 (Supporting information), the onset temperatures of weight loss (5%) were  $211\text{ }^\circ\text{C}$  for **BTPQ** and  $231\text{ }^\circ\text{C}$  for **BSPQ**.

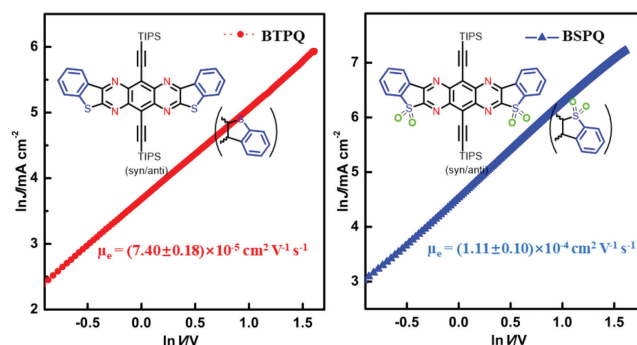


Fig. 5. The  $\ln J$ - $\ln V$  curve for **BTPQ** and **BSPQ**.

For further investigating the semiconductor properties and carrier mobility of the products, the space charge limited current method (SCLC) was used. The ITO/ZnO/active layer/Al structure was used to measure the electron mobility and hole mobility of the device, and the results were shown in Fig. 5. During the test process, the normal curve could not be obtained for the hole mobility, and the electron mobility of both devices gained ideal results in Fig. 5, which also verified that products **BTPQ** and **BSPQ** were n-type semiconductor materials. The electron mobility of **BTPQ** and **BSPQ** were  $7.40 \times 10^{-5}\text{ cm}^2\text{ V}^{-1}\text{ s}^{-1}$  and  $1.11 \times 10^{-4}\text{ cm}^2\text{ V}^{-1}\text{ s}^{-1}$ , respectively. Compared with the hole transport material **ABBT** derivatives, the properties of semiconductors changed from p-type to n-type with nitrogen atoms imported into molecular skeleton. The LUMO energy level of products decreased to a great extent, making product molecules easier to accept electrons. However, the electron mobility of sulfonated product **BSPQ** had been greatly improved by an order of magnitude. It could be ascribed to the obvious decrease of frontier orbital energy level through sulfonation. Especially, the LUMO energy level became more closer to the Fermi level, making the injection barrier reduced and more conducive to electron injection. Besides, the low-lying LUMO level ( $-4.1\text{ eV}$ ) could also prevent the influence of  $\text{H}_2\text{O}$  and  $\text{O}_2$ , which allowed the products and devices to exist stably in the air [38].

In summary, we have successfully constructed two novel air-stable n-type azaarenes with deep LUMO levels through two pathways. The appropriate introducing nitrogen atoms and sulfonyl group can not only increase the stability of the material but also fine modulate the frontier orbital energy levels, making the semiconductor properties change into n-type. Especially, sulfonation can favor the enhancement of electron mobility and make the products in the atmospheric environment unaffected.

#### Declaration of competing interest

The authors declare that they have no known competing financial interests or personal relationships that could have appeared to influence the work reported in this paper.

#### Acknowledgments

This work was supported by Natural Science Foundation of Heilongjiang Youth Fund (No. YQ2021B002), Heilongjiang Postdoctoral Scientific Research Developmental Fund (No. LBH-Q20018) State Key Laboratory of Urban Water Resource and Environment (Harbin Institute of Technology).

#### Supplementary materials

Supplementary material associated with this article can be found, in the online version, at doi:10.1016/j.ccl.2022.02.040.

## References

- [1] J. Li, Q. Zhang, *ACS Appl. Mater. Interfaces* 7 (2015) 28049–28062.
- [2] M. Müller, L. Ahrens, V. Brosius, et al., *J. Mater. Chem. C* 7 (2019) 14011–14034.
- [3] U.H.F. Bunz, J. Freudenberg, *Acc. Chem. Res.* 52 (2019) 1575–1587.
- [4] X. Shi, W. Kueh, B. Zheng, et al., *Angew. Chem. Int. Ed.* 54 (2015) 14412–14416.
- [5] P. Jin, T. Song, J. Xiao, et al., *Asian J. Org. Chem.* 7 (2018) 2130–2146.
- [6] C. Wang, J. Zhang, G. Long, et al., *Angew. Chem. Int. Ed.* 54 (2015) 6292–6296.
- [7] S. More, S. Choudhary, A. Higelin, et al., *Chem. Commun.* 50 (2014) 1976–1979.
- [8] Q. Miao, *Adv. Mater.* 26 (2014) 5541–5549.
- [9] A. Fukazawa, H. Oshima, S. Shimizu, et al., *J. Am. Chem. Soc.* 136 (2014) 8738–8745.
- [10] P. Gu, F. Zhou, J. Gao, et al., *J. Am. Chem. Soc.* 135 (2013) 14086–14089.
- [11] Z. Sun, Z. Zeng, J. Wu, *Acc. Chem. Res.* 47 (2014) 2582–2591.
- [12] G. Li, Y. Wu, J. Gao, et al., *J. Am. Chem. Soc.* 134 (2012) 20298–20301.
- [13] G. Li, Y. Wu, J. Gao, et al., *Chem. Asian J.* 8 (2013) 1574–1578.
- [14] Y. Wu, Z. Yin, J. Xiao, et al., *ACS Appl. Mater. Interfaces* 4 (2012) 1883–1886.
- [15] Z. Wang, P. Gu, G. Liu, et al., *Chem. Commun.* 53 (2017) 7772–7775.
- [16] J.T.E. Quinn, J. Zhu, X. Li, et al., *J. Mater. Chem. C* 5 (2017) 8654–8681.
- [17] A. Lakshminarayana, A. Ong, C. Chi, *J. Mater. Chem. C* 6 (2018) 3551–3563.
- [18] X. Gao, Y. Hu, *J. Mater. Chem. C* 2 (2014) 3099–3117.
- [19] X. Zhao, X. Zhan, *Chem. Soc. Rev.* 40 (2011) 3728–3743.
- [20] Y. Zhao, Y. Guo, Y. Liu, et al., *Adv. Mater.* 25 (2013) 5372–5391.
- [21] C. Wang, J. Zhang, G. Long, et al., *Angew. Chem. Int. Ed.* 54 (2015) 6292–6296.
- [22] J. Zaumseil, H. Siringhaus, *Chem. Rev.* 107 (2007) 1296–1323.
- [23] D.M. de Leeuw, M.M.J. Simenon, A.R. Brown, et al., *Synth. Met.* 87 (1997) 53–59.
- [24] H. Yan, Z. Chen, Y. Zheng, et al., *Nature* 457 (2009) 679–686.
- [25] F. Ding, D. Xia, W. Sun, et al., *Chem. Eur. J.* 25 (2019) 15106–15111.
- [26] F. Ding, D. Xia, C. Ge, et al., *J. Mater. Chem. C* 7 (2019) 14314–14319.
- [27] M. Chu, J. Fan, S. Yang, et al., *Adv. Mater.* 30 (2018) 1803467.
- [28] H. Pan, T. Song, X. Yin, et al., *Chem. Eur. J.* 24 (2018) 6572–6579.
- [29] M. Nandakumar, J. Karunakaran, A.K. Mohanakrishnan, *Org. Lett.* 16 (2014) 3068–3071.
- [30] S. Hahn, P. Biegger, M. Bender, et al., *Chem. Eur. J.* 22 (2016) 869–873.
- [31] M. Manassir, A.H. Pakiari, *J. Mol. Graph. Model.* 99 (2020) 107643–107649.
- [32] P. Hu, J. Ye, H. Jiang, *J. Mater. Chem. C* 7 (2019) 5858–5873.
- [33] D. Lehnerr, R. Hallani, R. McDonald, et al., *Org. Lett.* 14 (2012) 62–65.
- [34] L. Xu, Q. Zhang, *Sci. China Mater.* 60 (2017) 1093–1101.
- [35] C.K. Frederickson, M.M. Haley, *J. Org. Chem.* 79 (2014) 11241–11245.
- [36] H. Dong, C. Wang, W. Hu, *Chem. Commun.* 46 (2010) 5211–5222.
- [37] X. Zhan, A. Facchetti, S. Barlow, et al., *Adv. Mater.* 23 (2011) 268–284.
- [38] S. More, R. Bhosale, A. Mateo-Alonso, *Chem. Eur. J.* 20 (2014) 10626–10631.
- [39] Y. Min, C. Dou, H. Tian, et al., *Angew. Chem. Int. Ed.* 57 (2018) 2000–2004.